Tumor-Conditioned Macrophages Secrete Migration-Stimulating Factor: A New Marker for M2-Polarization, Influencing Tumor Cell Motility

Graziella Solinas,* Silvia Schiarea,† Manuela Liguori,* Marco Fabbri,*,‡ Samantha Pesce,* Luca Zammataro,* Fabio Pasqualini,* Manuela Nebuloni,§ Chiara Chiabrando,† Alberto Mantovani,*,¶ and Paola Allavena*

Tumor-associated macrophages (TAMs) are key orchestrators of the tumor microenvironment directly affecting neoplastic cell growth, neoangiogenesis, and extracellular matrix remodeling. In turn, the tumor milieu strongly influences maturation of TAMs and shapes several of their features. To address the early macrophage (Mϕ) differentiation phase in a malignant context, we mimicked a tumor microenvironment by in vitro coculturing human blood monocytes with conditioned media from different cancer cell lines. Only 2 out of 16 tumor cell lines induced Mϕ differentiation due to secreted M-CSF isoforms, including high molecular mass species. A global gene profiling of tumor-conditioned Mϕ was performed. Comparison with other datasets (polarized M1-Mϕ, M2-Mϕ, and TAMs isolated from human tumors) highlighted the upregulation of several genes also shared by TAM and M2-polarized Mϕ. The most expressed genes were selenoprotein 1, osteoactivin, osteopontin, and, interestingly, migration-stimulating factor (MSF), a poorly studied oncofoetal isoform of fibronectin. MSF (present in fetal/cancer epithelial and stromal cells but not in healthy tissues) was never identified in Mϕ. MSF production was confirmed by immunohistochemistry in human TAMs. MSF was induced by M-CSF, IL-4, and TGFβ but not by proinflammatory stimuli. RNA and protein analysis clearly demonstrated that it is specifically associated with the M2 polarization of Mϕ. Tumor-conditioned Mϕ-derived MSFs strongly stimulated tumor cell migration, thus contributing to the motile phenotype of neoplastic cells. In conclusion, MSF is a new molecule associated with the M2 polarization of Mϕ and expressed by TAMs. Its biological function may contribute to Mϕ-mediated promotion of cancer cell invasion and metastasis. ***The Journal of Immunology*****, 2010, 185: 642–652.**

Within the tumor context, macrophages (Mϕ) are increasingly recognized as pivotal regulators. High levels of tumor-associated Mϕ (TAMs) are often, even though not always, correlated with bad prognosis, and early and more recent studies have also highlighted a link between their abundance and the process of metastasis (1–7). This pathological evidence has been confirmed at gene level, where molecular signatures associated with poor prognosis in lymphomas and breast carcinomas include genes characteristic of Mϕ (e.g., CD68) and also in mouse models in which genetic ablation of Mϕ results in an inhibition of tumor progression and metastasis (8–10). TAMs carry out their proneoplastic role by influencing fundamental aspects of tumor biology: they produce molecules that directly affect neoplastic cell growth, motility, invasion, and intravasation, enhance neoangiogenesis, tune inflammatory responses and adaptive immunity, and catalyze important structural and substantial changes of the extracellular matrix (ECM) compartment (11–18). Interestingly, the transcriptome of TAMs (19) and of invasion promoting Mϕ has been recently analyzed, and these cells seem to represent a unique subpopulation having gene expression patterns related to tissue and organ development (20, 21). In addition, cells of hematopoietic origin have been shown to play a key role in the construction of a premetastatic niche (22–27).

As far as they have been studied, TAMs show mostly an M2-like phenotype (1, 16, 28). This preferential polarization is due to the absence in the tumor of M1-orienting signals such as IFN-γ or bacterial components as well as to the expression of M2 stimuli. Indeed, M2-Mϕ (or alternatively activated Mϕ) differentiate from monocytes due to specific growth factors (e.g., M-CSF) and post-stimulation with IL-4 and IL-13 (M2a), immune complexes/TLR ligands (M2b), or IL-10 and glucocorticoids (M2c) (28, 29). Of note, the infiltration of Th2 lymphocytes (driven by Th2-recruiting chemokines) has been reported in many tumors, and Th2 lymphocytes are a fundamental source of IL-4 and IL-13 cytokines (30–34). In general, hallmarks of M2-Mϕ are production of IL-10^{high}, IL-12^{low}, IL-1RA^{high}, IL-1decoyR^{high}, CCL17, and CCL22, high expression of mannose, scavenger and galactose-type receptors, poor Ag-presenting capability, wound healing promotion, scavenging of debris, angiogenesis, and tissue remodeling. Also, M2-polarized myeloid cells, as well as related myeloid

*Department of Immunology and Inflammation, Clinical Institute Humanitas, Rozzano; †Department of Environmental Health Sciences, "Mario Negri," Institute for Pharmacological Research; §Pathology Unit, L. Sacco Department of Clinical Sciences and ¶Department of Translational Medicine, University of Milan, Milan; and ‡Molecular Biology and Genomics Unit, European Commission's Joint Research Centre, Institute for Health and Consumer Protection, Ispra, Italy

Received for publication February 15, 2010. Accepted for publication April 22, 2010.

This work was supported by Associazione Italiana Ricerca Cancro Italy (to P.A. and A.M.) and grants from the Ministry of Health and Istituto Superiore Sanita Italy (Project Oncology 2006 and Alleanza Contro il Cancro).

Address correspondence and reprint requests to Dr. Paola Allavena or Prof. Alberto Mantovani, Department of Immunology and Inflammation, Istituto Di Ricovero e Cura a Carattere Scientifico Istituto Clinico Humanitas, Rozzano, Milan, Italy. E-mail addresses: paola.allavena@humanitasresearch.it or alberto.mantovani@humanitasresearch.it

Abbreviations used in this paper: CM, conditioned media; *Ct*, cycle threshold; ECM, extracellular matrix; ED, extra domain; FN, fibronectin; Gel-BD, gelatin-binding domain; LC-MS/MS, liquid chromatography tandem mass spectrometry; Mϕ, macrophage; MS/MS, tandem mass spectrometry; MSF, migration-stimulating factor; O/N, overnight; PCA, principal component analysis; rhM-CSF, recombinant human M-CSF; TAM, tumor-associated macrophage; TC-Mϕ, tumor-conditioned macrophage.

suppressor cells, wane the inflammatory/immune response by downregulating M1- and T cell-mediated functions (28, 35–40). On the contrary, inflammatory Mϕ (or classically activated or M1) originate upon stimulation with IFN-γ and microbial stimuli, such as LPS, and are characterized by IL-12^{high} and IL-23 production and consequent activation of polarized type I T cell response, cytotoxic activity, and good capability as APCs (28, 36–39).

Molecular mechanisms underlying Mϕ polarization remain scanty. Tuning of NF-κB activation by p50 homodimers has been associated with M2 differentiation (41, 42). Peroxisome proliferator activated receptor γ is involved in the M2-like differentiation (43–46), and the phosphatase SHIP was shown to play a key role in balancing Mϕ polarization, although recent evidence suggests that it may act indirectly through the regulation of IL-4 production by basophils (47). Recently, Pienta and colleagues (48) reported that CCL2 and IL-6 sustain the survival of myeloid cells at the tumor site and support their differentiation toward tumor-promoting M2-Mϕ.

Tumor Mϕ are considered attractive targets of anti-cancer strategies. To this end, the first step should be the identification of molecules specifically overexpressed or produced by TAMs but neither by resident Mϕ of distant healthy tissues nor by M1 cells, which are important to face pathogens and could take part in anti-cancer actions.

In this study, we focused our work on the initial differentiation phase of monocytes to identify molecules upregulated by Mϕ within the tumor context. To mimic a tumor microenvironment, blood monocytes were in vitro exposed to cancer cell-conditioned media. Differentiated Mϕ, named tumor-conditioned Mϕ (TC-Mϕ), were analyzed for phenotype, functional activity, cytokine/chemokine production, and gene expression.

In this study, we report that TC-Mϕ have a gene expression pattern similar to that of TAMs. Among these genes, we focused on a truncated isoform of fibronectin (FN), migration-stimulating factor (MSF), which is potently chemotactic for tumor cells. We provide evidence that MSF is produced by M2-Mϕ and TAMs and therefore may be considered as a novel marker for M2 polarization.

Materials and Methods

Cell line cultures and tumor-conditioned media preparation

Human ovarian cancer cell lines Ovcar3 and A2780, human colon cancer cell lines HT29, HCT-116, LoVo-N, CaCo-1, and SW620, human pancreatic carcinoma cell lines PaCa44, PaCa3, CFPAC, PC, T3M4, PT45, Panc1, MiaPaCa2, and AsPC1, and the immortalized normal pancreatic epithelial cell line HPDE6 were cultured in RPMI 1640 (Lonza, Basel, Switzerland) supplemented with 10% FBS. Once grown to 90% of confluence, media were discarded, and flasks were rinsed two times with saline solution. Cells were then incubated with fresh RPMI for 24 h; the conditioned media (CM) was collected and filtered at 0.20 μm, and the supernatant was stored at −20°C. All cell lines were routinely checked for *Mycoplasma* contamination.

Mϕ and TC-Mϕ differentiation

Human monocytes were obtained from normal blood donor buffy coats by two-step gradient centrifugation, first by Histopaque-1077 (Sigma-Aldrich, Milan, Italy) and then by Percoll (GE Healthcare, Milan, Italy) (49). Residual T and B cells were removed from monocyte fraction by plastic adherence.

Mϕ and TC-Mϕ were obtained by culturing 10^6/ml monocytes for 6 d in RPMI 1640 5% FBS supplemented with 25 ng/ml of recombinant human M-CSF (rhM-CSF; PeproTech, Milan, Italy) or in the presence of 30% of tumor cell line supernatants (TC-Mϕ). All culture reagents contained <0.125 endotoxin unit/ml as checked by *Limulus* amebocyte lysate assay (BioWhittaker, Walkersville, MD).

M1- and M2-polarized Mϕ were obtained by culturing 10^6/ml monocytes for 6 d in RPMI 1640 5% FBS with 25 ng/ml rhM-CSF. M1 cells were polarized by stimulating overnight (O/N) M-CSF Mϕ with LPS (100 ng/ml) (PeproTech) and IFN-γ (500 U/ml) (PeproTech). M2-Mϕ were polarized by stimulating O/N M-CSF Mϕ with IL-4 (20 ng/ml) (PeproTech).

Isolation of human TAMs

Human TAMs were isolated from solid tumors of untreated patients with histologically confirmed epithelial ovarian carcinoma admitted to the Department of Obstetrics and Gynecology, San Gerardo Hospital (Monza, Italy). Briefly, solid tumors were enzymatically digested and centrifuged over Ficoll as described (41). Tumor Mϕ were isolated by plastic adherence (RPM1 1640 without FBS, 1 h, 37°C). The adherent cells were >95% Mϕ as assessed by morphology and CD68 positivity. All culture reagents contained <0.125 endotoxin unit/ml as checked by *Limulus* amebocyte lysate assay (BioWhittaker).

M-CSFR blockade

To block M-CSFRs, monocytes were incubated with 2 μg/ml anti–M-CSFR (Santa Cruz Biotechnology, Tebu-bio, Milan, Italy) for 30 min at 37°C or with an anti-human IgG irrelevant Ab 10 μg/ml (Sigma-Aldrich).

Tumor-derived M-CSF neutralization

To neutralize tumor-derived M-CSF, Panc1-CM was incubated for 20 min with different concentrations of Recombinant Human M-CSF R-Fc Chimera (Symansis, Auckland, New Zealand). As experimental control, a solution of rhM-CSF 25 ng/ml was treated following a similar protocol.

Chemotaxis

Cell migration was evaluated using transwell systems with 5 μm (for monocytes) or 8 μm (for Panc1 tumor cells) pore size (Costar, Euroclone, Milan, Italy). CM from TC-Mϕ or M1- and M2-Mϕ were prepared after 6 to 7 d of differentiation as described above. Medium was replaced with fresh medium and supernatants collected after 24 h. Mϕ supernatants or recombinant human MSF (kind gift of Prof. Schor, University of Dundee, Scotland, U.K.) were used as chemoattractants in the lower compartment. To block gelatin-binding domain (Gel-BD), tumor-conditioned supernatants were pretreated for 30 min at room temperature with anti–Gel-BD Ab (Chemicon, Milan, Italy), 10 μg/ml. Results are expressed as the mean number of migrated cells counted in 10 microscope high-power fields (magnification ×1000) after 18 h. Each experiment was performed in triplicate. The p value was calculated by Student t test.

Real-time RT-PCR

Total RNA extraction from monocytes, in vitro-cultured Mϕ, and TAMs isolated from human tumors was performed with TRIzol (Invitrogen, Milan, Italy). cDNA was synthesized by random priming from 1 μg total RNA with the GeneAmp RNA PCR kit (Applied Biosystems, Monza, Italy) according to the manufacturer's instructions. Real-Time PCR was performed using SYBR Green dye and 7900HT Fast Real Time PCR Systems (Applied Biosystems). The sequences of primer pairs specific for each gene (Invitrogen) were designed with Primer Express Software (Applied Biosystems) and were as follows: human CSF-1 isoform A (5′-GCC ATC CCT AGC AGT GAC C-3′ and 5′-TCA AAG GAA CGG AGT TAA AAC GG-3′); human CSF-1 isoform B (5′-GCG AGC AGG AGT ATC ACC G-3′ and 5′-CCC TCA GTT CCC TCA GAG TC-3′); human CSF-1 isoform C (5′-GCT CTC CCA GGA TCT CAT CAC-3′ and 5′-AGG TCT CCA TCT GAC TGT CAA T-3′); GAPDH (5′-AGA TCA TCA GCA ATG CCT CCT G -3′ and 5′-ATG GCA TGG ACT GTG GTC ATG-3′); FN (5′-ATC AAC CTT GCT CCT GAC AG-3′ and 5′-GTC TCA GTA GCA TCT GTC AC-3′); MSF (5′-GCA TTG CCA ACC TTT ACA GAC-3′ and 5′-TTT CTG GGT GGG ATA CTC AC-3′); extra domain (ED)-A (5′-CGG GAT CCA ACA TTG ATC GCC CTA AAG G-3′ and 5′-TCC CCC GGG TGT GGA CTG GGT TCC AAT C-3′); and ED-B (5′-CAA GGA TGA CAA GGA AAG TG-3′ and 5′-AAT AAT GGT GGA AGA GTT TAG C-3′). A total of 2 μl cDNA was used as the template; 12.5 μl 2× SYBR Green PCR Master Mix (Applied Biosystems) was mixed with template and primers. The total reaction volume was 25 μl. Cycling conditions were 10 min at 95°C, 40 cycles of 15 s at 95°C, and 1 min at 60°C. Experiments were performed in triplicate for each sample. mRNA was normalized to GAPDH mRNA by subtracting the cycle threshold (Ct) value of GAPDH mRNA from the Ct value of the gene (ΔCt). Fold difference ($2^{-\Delta\Delta Ct}$) was calculated by comparing the ΔCt with the ΔCt of the AsPC1-Mϕ.

Transcriptional profile analysis

Monocytes from three independent donors were stimulated as described above with tumor CM for 4 or 72 h. Total RNA was extracted from 5×10^6 cells using TRIzol (Invitrogen/Life Technologies), retrotranscribed, and prepared for GeneChip hybridization as previously described (41). Fragmented cRNA was hybridized to Affymetrix HG-U133 Plus 2.0 GeneChips

(Affymetrix, Santa Clara, CA), then washed and scanned according to the manufacturer's guidelines. Expression measures were computed using robust multiarray average. Principal component analysis (PCA) was carried out on all genes analyzed to assign the general variability in the data to a reduced set of variables called principal components. Available were datasets of human TAMs (three different donors) and datasets from M1- and M2-polarized Mϕ.

PCA (analysis was applied to the complete dataset) is a mathematical algorithm that reduces the dimensionality of the data. It accomplishes this reduction by identifying directions, called principal components, along which the variation in the data is maximal.

In PCA, we obtain a set of orthogonal axes oriented in the directions of largest variance within a set of data points in a high-dimensional space. The first principal component is a vector in the direction of greatest variance, the second principal component is a vector in the direction of greatest variance orthogonal to this, and so on. These vectors are in fact eigenvectors of the empirical data covariance matrix. Values on the *x*- and *y*-axis express a two-dimensional representation of greatest variance vectors (50).

Technical information requested by Minimum Information about a Microarray Experiment of the latter is available at the Gene Expression Omnibus Web site (www.ncbi.nlm.nih.gov/geo) under the accession number GSE5099. Statistical differences were assessed by a moderated *t* test analysis performed using a limma bioconductor package, and resulting *p* values were adjusted using the Benjamini and Hochberg step-up method for controlling the false discovery rate. Genes were defined as regulated when characterized by a fold of induction ≥ 2 and a false discovery rate *p* value ≤ 0.05. Computations were conducted using the R statistics programming environment (available at www.r-project.org). Gene trends were organized by K-means clustering using squared Pearson correlation with the TIGR MultiExperiment Viewer (www.tm4.org/). Single-gene comparison was performed by analyzing the relative expression to median value (1) calculated among four Affymetrix datasets (TC-Mϕ, M1, M2, and TAM).

ELISA

Cytokine production in tumor cell and Mϕ supernatants was measured by commercially available ELISA kits (IL-10, IL-12, CCL2, CCL17, IL-6, IL-8, TNF-α) according to the manufacturer's instructions (R&D Systems, Space Import, Milan, Italy). Mϕ were stimulated or not with LPS (100 ng/ml) (PeproTech) for 24 h.

Bio-Plex Protein Array System

M-CSF in tumor cell line supernatants was measured using the Bio-Plex Protein Array System (Bio-Rad, Milan, Italy) according to the manufacturer's instructions.

Western blot

Because there are no commercially available reagents for MSF, we kindly received anti-MSF Abs from Prof. Schor (University of Dundee). Rabbit polyclonal anti-MSF Ab (raised against a synthetic peptide containing the MSF-specific C-terminal decapeptide sequence) was used diluted 1:10,000. Protein extracts were processed as described (19).

Flow cytometry

In vitro-differentiated Mϕ were analyzed by flow cytometry on FACS-Canto (BD Biosciences, Milan, Italy). Human FcRs were blocked using PBS 1% human serum. For staining, cells were washed and resuspended in FACS buffer (PBS 0.5% BSA, 0.05% NaN_3). PE-mouse anti-human CD16, APC-mouse anti-human CD14, FITC-mouse anti-human mannose receptor CD206, and PE-mouse anti-human CD68 were obtained from BD Biosciences. For the CD68 staining, we used the BD Fixation/Permeabilization solution kit (BD Biosciences).

Immunohistochemistry

Human surgical samples of pancreatic and ovarian tumors were fixed in 10% buffered formalin for 24–48 h and embedded in paraffin. Sections were cut, mounted on Superfrost slides (BioOptica, Milan, Italy), dewaxed in xylene, rehydrated in ethanol, and pretreated in a microwave oven (two cycles for 3 min each at 800 W in 0.25 mM EDTA buffer). Double immunohistochemistry was performed with anti-human CD68 (clone KP1, Dako, Glostrup, Denmark; 1:100 to detect Mϕ) and anti-human MSF Ab (mAb clone 7.1, 1:100; Prof. Schor, University of Dundee). Specific secondary Abs conjugated with alkaline phosphatase (Biocare Medical, Concord, CA) for CD68 and ARK peroxidase (Dako) were used. The first reaction (anti-CD68) was developed by using Ferranji blue (blue-stained) and the second (anti-MSF) by using 3,3′-diaminobenzidine–free base as chromogen (brown-stained). For the second staining, double immunohistochemistry was performed with anti-human CD68 (clone KP1, Dako; 1:100 to detect Mϕ) and rabbit polyclonal anti-human MSF Ab (homemade, raised against a synthetic peptide containing the MSF-specific C-terminal decapeptide sequence; diluted 1:100). Mach2 double stain 1 (Biocare Medical) was used to detect mouse primary Ab in alkaline phosphatase and rabbit primary Ab in peroxidase. The first reaction (CD68) was developed by using Ferranji blue (blue-stained; Biocare Medical) and the second by using diaminobenzidine as chromogen (brown-stained; Biocare Medical); nuclei were counterstained with Nuclear Fast Red (BioOptica, Milan, Italy).

Global proteomic analysis of CM

A proteomic analysis was performed on serum-free CM of tumor cell lines (PT45, Panc-1, MiaPaCa2, ASPC1) (S. Schiarea, G. Solinas, P. Allavena, G.M. Scigliuolo, R. Bagnati, R. Fanelli, C. Chiabrando, submitted for publication). CM was concentrated using 5-kDa molecular mass cut-off centrifugal filter devices (Millipore, Bedford, MA). Proteins were separated by one-dimensional SDS-PAGE in reducing conditions on 4–12% NuPAGE Bis-Tris gel (Invitrogen). Each gel lane was cut into 24 bands of equal height. Proteins in each bands were reduced, alkylated, and in-gel digested with bovine trypsin. Digests were analyzed by liquid chromatography tandem mass spectrometry LC-MS/MS with a high-resolution/high-accuracy mass spectrometer (LTQ Orbitrap XL, Thermo Fisher Scientific, Waltham, MA). Tandem MS/MS data were analyzed with Mascot version 2.2 (Matrix Science, Boston, MA) against the Swiss-Prot database, version 56.5 (http://us.expasy.org/sprot/download.html).

Results

Effects of tumor cell line conditioned-media on human monocytes

To mimick a tumor microenvironment, we exposed human blood monocytes to tumor cell CM, in the absence of other exogenous stimuli. We tested several CM from different tumor cell lines (five from colorectal cancer, two from ovarian cancer, and nine from pancreatic carcinoma) and noticed that only those from the pancreatic cancer cell lines PT45 and Panc1 were able to induce evident morphological modifications of monocytes. Therefore, we decided to restrict our investigation to these active cell lines, using as negative controls other pancreatic (cancer or normal) cell lines without differentiating activity (i.e., AsPC1 and MiaPaCa2) and the normal human pancreatic ductal epithelial cell line HPDE6. The CM from PT45 or Panc1 as well as rhM-CSF induced a strong differentiation of monocytes that became larger, with ruffling membrane typical of Mϕ, whereas the majority of monocytes cultured with AsPC1-, MiaPaCa2-, and HPDE-CM almost completely died. Representative images of the cultured cells are shown in Fig. 1*A*. We confirmed by FACS analysis that the differentiation of monocytes (evaluated as percentage of large cells, side scatter) was strongly induced by rhM-CSF ($46.77 \pm 8.8\%$) and PT45- ($41.62 \pm 2.55\%$) or Panc1-CM ($36.24 \pm 2.7\%$). In contrast, only minimal monocyte differentiation was induced by other CM, as well as by RPMI without additions ($6.35 \pm 1.18\%$) (Fig. 1*B*). Mϕ differentiated by tumor-CM were defined in this study as TC-Mϕ.

To study the phenotype of the differentiated cells, we assessed the expression of CD14, CD16, CD68, and mannose receptor. All of these molecules were highly expressed by Mϕ cultured with rhM-CSF as well as by Mϕ differentiated in the presence of PT45- and Panc1-CM (Fig. 1*C*). The dendritic cell marker CD1a was completely absent from TC-Mϕ, thus excluding that tumor-CM were inducing a dendritic cell-like differentiation (data not shown). To better characterize the differentiated cells, we measured the constitutive and LPS-stimulated release of cytokines/chemokines by rhM-CSF-Mϕ, TC-Mϕ, and TAMs directly isolated from human tumor. In particular, Panc1-CM induced expression of IL-10, IL-6, and TNF-α and high amounts of CCL2 by Mϕ. Similarly, PT45-Mϕ produced IL-6 and TNF-α and very high quantities of IL-10 and CCL2. Notably, neither Panc1-Mϕ nor PT45-Mϕ produced

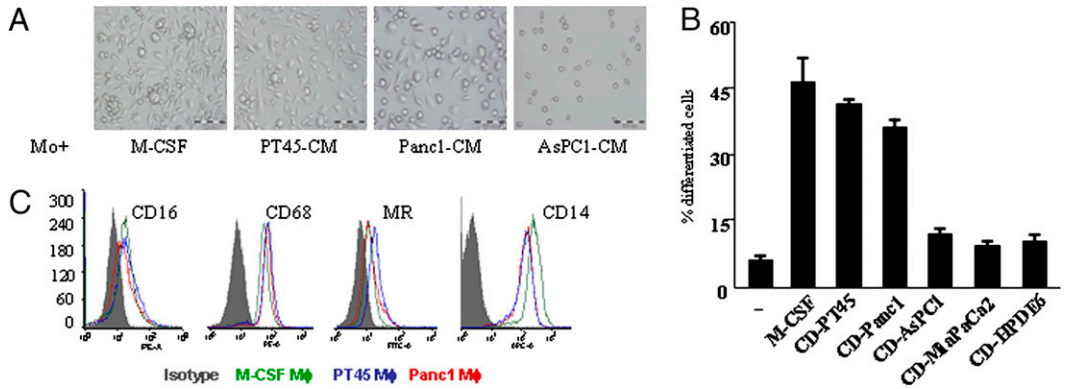

FIGURE 1. Effects of tumor-CM on human monocyte differentiation. Human monocytes were cultured in the presence of 30% v/v of tumor cell line-CM in the absence of exogenous stimuli or with 25 ng/ml M-CSF. *A*, Representative images of cell cultures at day 6. PT45 and Panc1-CM induced monocyte to Mϕ differentiation. *B*, Flow cytometry. Percentage of large gated cells over total input monocytes evaluated as side scatter. Mean ± SD of >10 experiments. *C*, Phenotype analysis of TC-Mϕ.

IL-12, even after LPS stimulation. The cytokine/chemokine production profiles of TC-Mϕ were similar to those of freshly isolated human TAM (Table I).

Identification of monocyte-differentiating bioactivity in tumor-CM

We first established whether the monocyte to Mϕ-differentiating activity observed in the two active cell lines was due to the known growth factor, M-CSF. Bio-Plex Protein Array System (Bio-Rad) analysis determined 600 ± 0.01 pg/ml of M-CSF in the active cell line PT45 and 200 ± 0.11 pg/ml in Panc1 and undetectable levels in the inactive cell lines AsPC1 and MiaPaCa2. As M-CSF is known to exist in separable isoforms with different m.w. (a secreted glycoprotein, a high molecular mass secreted proteoglycan, and a membrane-spanning cell-surface glycoprotein) (51), mRNA levels with primers specific for the three isoforms were tested. The results confirmed a much higher overall expression of M-CSF species in the active than in the inactive cell lines (Fig. 2*A*). Evidence of the prevalent secretion of high molecular mass M-CSF isoforms was suggested, in an independent study, by a mass spectrometry-based proteomic analysis on the secretome of pancreatic cancer cell lines, in which several M-CSF peptides were identified in PT45 and Panc1 (but not Aspc1 and MiaPaca2). M-CSF peptides mostly belonged to molecular species migrating at high molecular mass (>100 kDa) in reducing SDS-PAGE, likely representing proteoglycan isoform subunits (S. Schiarea, G. Solinas, P. Allavena, R. Fanelli, C. Chiabrando, personal communication).

To verify that tumor-derived M-CSF was the major factor responsible for the differentiation of monocytes, we neutralized its activity with specific reagents. Depletion of M-CSF in tumor-CM with a soluble M-CSFR caused a marked reduction of its differentiating activity (Fig. 2*B*). In addition, blocking M-CSFRs on monocytes with a specific Ab made these cells completely insensitive to the differentiating activity of PT45- and Panc1-CM (Fig. 2*C*). Of interest, IL-34, the other only known specific ligand of the M-CSFR, was not identified in the above-cited proteomic analysis of tumor-CM. Taken together, these results demonstrate that the differentiating activity of the active tumor-CM was exclusively due to M-CSF molecular species.

Profiling of upregulated genes expressed by TC-Mϕ

To obtain a comprehensive view of our TC-Mϕ, we performed a gene expression analysis. Two time points were considered: 4 and 72 h. After 4 h culture, only 12 genes were upregulated (>2-fold) versus resting monocytes. Among these were three chemokines (*CCL2, CCL7*, and *CXCL1*), *COX-2*, the β form of pro-IL-1, and vascular endothelial growth factor (not shown).

A summary of the results of expressed genes at 72 h culture is shown in Table II. Overall, >500 genes had >2-fold expression and 20 genes had >10-fold expression relative to resting monocytes. Several upregulated genes were characteristic of the M2-Mϕ polarization: the mannose receptor (*CD206*), other members of the C-type lectin R family (e.g., *MGL/CLEC10/CD301, CLEC11* and *DCL-1/CD302*, and *CD209*), the receptors for the Fc fragment of IgG (*CD32* and *CD64*), and receptors importantly implicated in the uptake of extracellular macromolecules and scavenging of debris, like *SR-A, SR-B, CD163*, and *stabilin-1* (*STAB1*). The latter is a membrane receptor involved in the binding/scavenging of the matricellular protein secreted acidic and rich in cysteine (52).

The most expressed genes were selenoprotein (*SEPP1*) with a 95-fold and osteoactivin (*OA*) with an 83-fold expression. Other upregulated molecules related to the ECM were fibronectin (*FN1*), *F13A1*, which catalyses the polymerization of several matrix proteins, and osteopontin (*OPN*). A set of mRNA coding for adhesion molecules was enhanced; these include integrin β5,

Table I. *Protein levels produced by TC-Mϕ and TAM (ng/ml)*

	M-CSF–Mϕ		Panc1-Mϕ		PT45-Mϕ		TAM	
	LPS −	LPS +	LPS −	LPS +	LPS −	LPS +	LPS −	LPS +
IL-10	0.13 ± 0.04	0.93 ± 0.06	<0.01	0.82 ± 0.14	<0.01	2.36 ± 0.39	0,10 ± 0.00	2.83 ± 0.03
IL-12	0.03 ± 0.01	0.42 ± 0.11	<0.01	0.01 ± 0.00	0.01 ± 0.00	0.01 ± 0.00	0.01 ± 0.02	0.02 ± 0.01
CCL2	6.08 ± 2.75	6.46 ± 1.18	5.36 ± 1.55	8.25 ± 2.30	3.63 ± 1.09	12.40 ± 3.28	12.10 ± 5.4	20.03 ± 1.18
IL-6	<0.01	0.24 ± 0.05	<0.01	0.31 ± 0.05	0.02 ± 0.01	1.32 ± 0.27	12.5 ± 3.5	65 ± 0.23
TNF-α	<0.01	1.13 ± 0.34	0.01 ± 0.00	1.05 ± 0.46	<0.01	1.83 ± 0.47	0.1 ± 0.04	12.6 ± 0.53

Protein levels of chemokines and cytokines produced by TC-Mϕ and TAM with and without LPS (mean ± SD of 2–4 experiments).

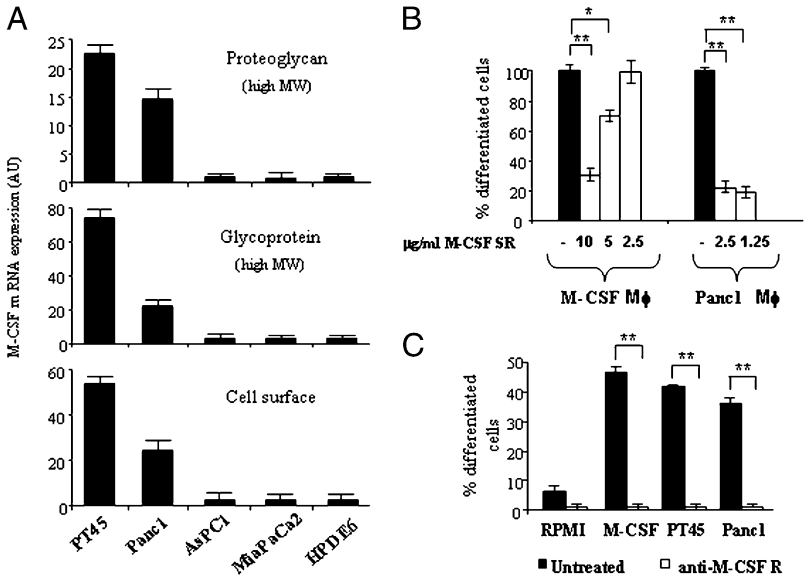

FIGURE 2. M-CSF involvement in TC-Mϕ differentiation. *A*, mRNA expression of different M-CSF isoforms in pancreatic tumor cell lines and in HPDE6 cells. *B*, Monocytes cultured with 30% v/v of tumor-CM pretreated with different concentrations of rhMCSF R-Fc Chimera (Symansis). Results from one representative experiment of three performed. *C*, Monocytes pretreated with blocking M-CSFR Ab cultured with 30% v/v of tumor-CM. Results from one representative experiments of three performed. $*p \leq 0.05$; $**p \leq 0.01$.

the *VLA-4*, P selectin ligand, *CD81* (also involved in cell motility as well as cell activation and signal transduction), two sialic-acid binding proteins (*Siglec1* and *Siglec7*), and *SLAMF8*. Highly expressed (22-fold) was the gene coding for the myelin-associated protein (*PMP22*), a binding partner in the integrin/laminin complex and specifically binding α6 β4.

Table II. *Gene expression analysis of TC-Mϕ*

Family	Symbol	Description	Fold Increase
C-type lectin R	*MRC1*	Mannose receptor/CD206	44
	CD209	DC-SIGN	3.6
	CD302	DCL-1	3
	CLEC10A	MGL/CD301	2.5
Fcγ receptors	*FCGR2B*	CD32	10
	FCGRT	Fc for IgG transporter	4
	FCGR1A	CD64	2.5
Scavenging receptors	*MSR1*	Scavenger receptor, SR-A	9
	STAB1	Stabilin1/SPARC-R	6
	CD163	CD163	5
	SCARB1	Scavenger R, class B	3
ECM molecules	*GPNMB*	OA	83
	SPP1	OPN	26
	F13A1	Factor XIII A1	11
	FN1	Fibronectin	7
Adhesion molecules and related	*PMP22*	Myelin-associated protein	22
	SIGLEC1	Sialoadhesin 1	12
	SLAMF8	CD2 family member	11
	ITGB5	β5 integrin	3.5
	CD81	CD81	3
	SIGLEC7	Sialoadhesin 7	2.7
	SELPLG	P selectin ligand	2.5
	ITGA4	α4 subunit, VLA4	2.1
Enzymes	*ADAMDEC1*	Decysin	7
	CPM	Carboxipeptidase	6
	MMP9	MMP9	6
	ADAM28	ADAM28	4
	PLAU	uPA	4
	MMP2	MMP2	3
MHC molecules and related	*HLA-DMA*	HLA-DMA	5
	CIITA	MHC IL, transactivator	3
	CTSC	Cathepsin C	9
	CTSD	Cathepsin D	4
	CTSB	Cathepsin B	3
	CTSK	Cathepsin K	2.01
Protein trafficking	*VPS45*	Vacuolar sorting protein	5
	VPS13B	Vacuolar sorting protein	3.01
	LAMP1	Lysosomal protein 1	3
	LAMP2	Lysosomal protein 2	3
Miscellaneous	*SEPP1*	Selenoprotein 1	95

Human monocytes were stimulated for 72 h with tumor-CM. Results (mean of three different donors) are fold-increase relative to unstimulated monocytes.

A large number of protease genes were strongly expressed and included: *CPM*, *MMP2* and *MMP9*, and ADAM molecules, such as decysin, *ADAM28*, and *uPA*. Other proteolytic enzymes whose expression was enhanced were the cysteine proteases (cathepsins type C, D, A, B, and K). These molecules are extremely important for the maturation of the MHC class II molecules and for the correct loading of antigenic peptides. The genes coding for the *trans*-activator of HLA class II *CIITA* and genes of the HLA-II family were also increased, especially *HLA-DMA*. Other expressed mRNA code for proteins involved in the trafficking and sorting of molecules within specific organelles: *VPS45* and *VPS13B* as well as lysosomal-associated membrane proteins (*LAMP1* and *LAMP2*).

To broaden our study, we compared the expression of some upregulated genes of TC-Mϕ with that of TAMs isolated from human tumors and of in vitro M1- and M2-polarized Mϕ performed in our laboratory with the same Affymetrix technology (53). Some upregulated genes in TC-Mϕ were similarly expressed in TAM and to a further extent in M2-Mϕ but not in M1-polarized cells (Fig. 3*A*).

From this restricted gene comparison, we moved to a global gene profiling comparison of TC-Mϕ, TAM, M1, and M2 cells. To identify sources of variability among these entire databases, a PCA was performed (50, 54, 55).

This PCA showed that TC-Mϕ are indeed comparable to TAMs, and this observation confirmed the validity of our in vitro tumor-conditioning model of Mϕ differentiation. Moreover, their global profiling is closer to that of M2- than M1-polarized Mϕ (Fig. 3*B*). Finally, these data boosted the concept of the M2-like polarization for TAMs.

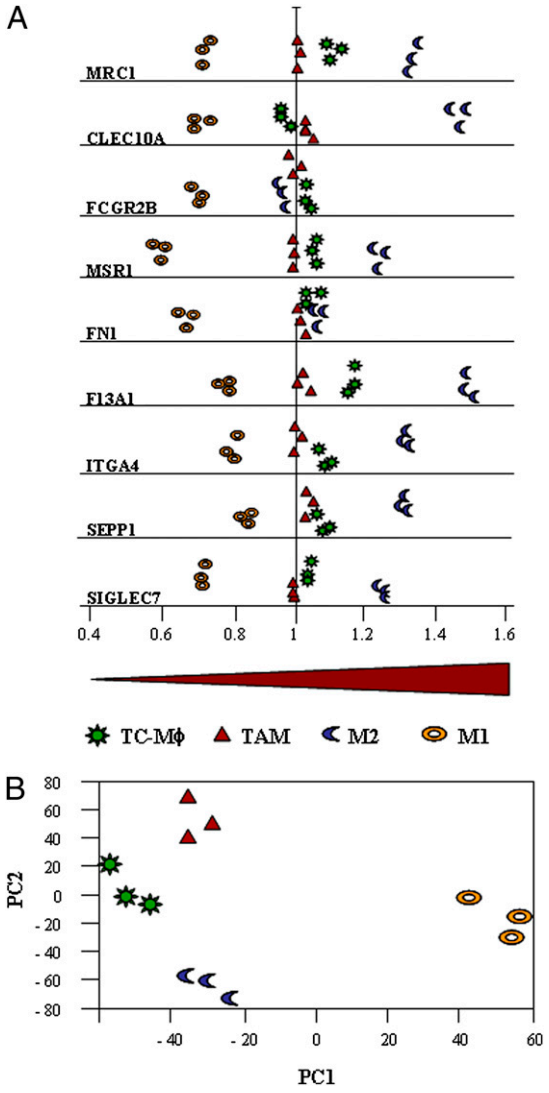

FIGURE 3. Global gene profiling comparison among TC-Mϕ, TAM, M1-, and M2-polarized cells. *A*, *MRC1*, *CLEC10A*, *FCGR2B*, *MSR1*, *FN1*, *F13A1*, *ITGA4*, *SEPP1*, and *SIGLEC7* were similarly expressed in TC-Mϕ and TAM and more expressed in Mϕ with an M2 phenotype compared with M1-polarized cells. Results are presented as relative expression to median value (1) of genes calculated among four Affymetrix datasets. *B*, Global gene profiling comparison performed among the TC-Mϕ, TAM, M1, and M2 dataset by PCA. The results show that M1 and M2 cells are distinct in terms of global gene expression. TC-Mϕ are more closely related to TAM and M2-polarized Mϕ.

Fibronectin isoforms in TC-Mϕ

The mRNA profiling revealed that the *FN1* gene was highly expressed in TC-Mϕ. Alternative splicing within human FN pre-mRNA results in the generation of ~20 distinct isoforms (56–59). Because specific isoforms of FN are known to contribute to cancer pathogenesis (60, 61), we decided to further investigate their possible expression in TC-Mϕ.

Using primers specific for distinct domains, we tested in TC-Mϕ the expression of four FN isoforms: full-length FN, oncofetal ED-A FN, oncofetal ED-B FN, and MSF. We found that the most abundant FN mRNA transcripts expressed by TC-Mϕ were the full-length isoform and the MSF (Fig. 4*A*). MSF differs from the other two oncofetal full-length isoforms because it is identical to their 70-kDa N terminus but terminates in a unique 10 aa sequence, and it has been defined as a truncated isoform (62). Importantly, MSF was known to be produced by fibroblasts, fetal skin keratinocytes, tumor cells, and tumor-associated vascular endothelial cells (62) but not by Mϕ. We observed an opposite trend over time for the MSF expression compared with full-length FN. The TC-Mϕ MSF mRNA level increased along with either the time of culture and the number of supernatant stimuli, whereas transcripts from the full-length FN decreased (Fig. 4*B*, 4*C*).

Next, we investigated whether MSF was preferentially associated with the classically (M1) or alternative (M2) Mϕ polarization. By analyzing 6-d in vitro rhM-CSF–differentiated Mϕ, further polarized with LPS/IFN-γ or IL-4, it was evident that MSF expression was higher in M2-Mϕ compared with M1 cells (Fig. 4*D*). Moreover, MSF expression was specifically associated with M2 cells because its levels were dramatically downregulated in M2 cells reverted into M1 (with LPS/IFN-γ) and, on the contrary, strongly upregulated in M1 cells skewed toward the M2 phenotype (with IL-4) (Fig. 4*D*). Higher MSF production in M2-Mϕ was confirmed at protein level by Western blot as shown in Fig. 4*E*.

To confirm MSF expression by tumor-infiltrating leukocytes in vivo, we performed RT-PCR with purified ex vivo preparations of TAM. Four different preparations isolated from human ovarian carcinoma specimens expressed MSF transcripts (Fig. 5*A*). In addition, immunohistochemical analysis of tumor sections showed that immunoreactivity for anti-MSF was detected in $CD68^+$ cells infiltrating human tumors (Fig. 5*B*).

To better understand the regulation of MSF in myeloid cells, we stimulated human monocytes with several cytokines and growth factors for 24 h. Interestingly, we noticed unequivocally different effects between inflammatory and anti-inflammatory stimuli. As shown in Fig. 6*A*, M-CSF, IL-4, and especially TGFβ strongly promoted MSF production, whereas LPS, TNF-α, and IFN-γ did not. As TGFβ was almost undetectable in our tumor-CM, we checked the effect of the natural tumor-derived M-CSF. Pretreatment of monocytes with anti–M-CSF Ab almost completely abrogated MSF expression, indicating that, in our experimental conditions, M-CSF is

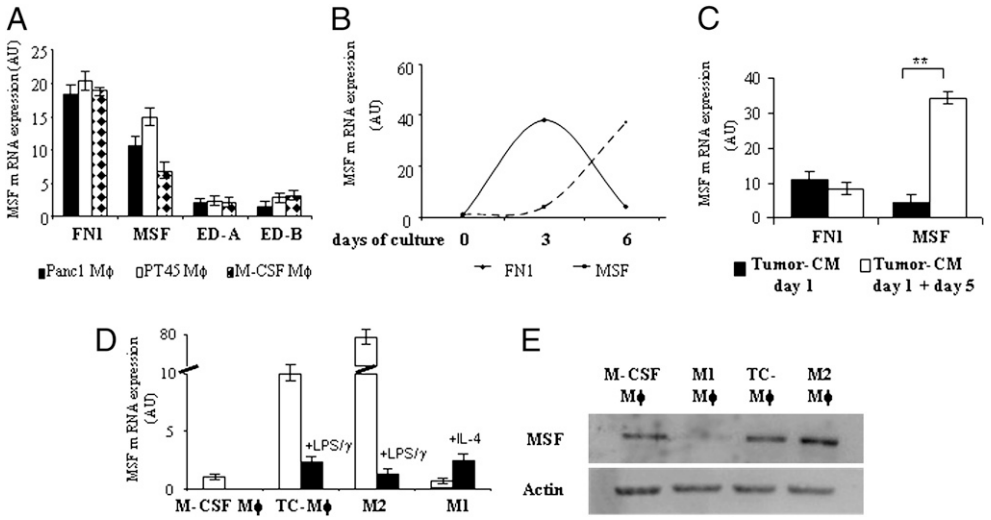

FIGURE 4. Expression of MSF in TC-Mϕ. *A*, mRNA level expression of full-length *FN1*, ED-A FN, ED-B FN, and MSF. MSF and full-length *FN1* in TC-Mϕ at different times of culture (days 0, 3, 6) (*B*) and upon repeated stimulation (days 1 and 5) with tumor-CM (*C*). D, MSF mRNA levels in Mϕ polarization (white bars). M1 stimuli: LPS + IFN-γ; M2 stimulus: IL-4. Black bars indicate MSF expression in reverted Mϕ treated as indicated. *E*, Western blot analysis of MSF production in TC-Mϕ, M-CSF-Mϕ, M1-, and M2-polarized Mϕ. $**p \leq 0.01$.

the main tumor-derived factor able to induce MSF expression in monocytes (Fig. 6*B*).

Functional characterization of MSF

It has been reported that MSF has chemotactic activity for fibroblasts and tumor cells through its Gel-BD domain. We confirmed these results with the tumor cell line Panc1 and human monocytes (Fig. 7*A*, 7*B*). Of note, MSF showed its maximal chemotactic activity at picomolar concentrations; whereas monocyte migration peaked at 1 to 2 ng/ml, tumor cells responded at 10-fold less MSF concentration.

We next determined the chemotactic activity of MSF released by TC-Mϕ and M2-polarized Mϕ. Fig. 7*C* demonstrates that supernatants from both Mϕ populations, but not from M1 cells, did stimulate tumor cell migration. Inhibition of MSF with a specific anti-MSF Ab directed to the Gel-BD (62) reduced the number of migrated tumor cells, thus demonstrating the specific involvement of MSF (Fig. 7*D*).

Discussion

The major focus of this study was to clarify how the malignant context is able to influence the fundamental initial phase of monocyte to Mϕ differentiation. We mimicked a tumor microenvironment by exposing human blood monocytes to tumor cell CM in the absence of other exogenous stimuli. Only 2 out of the 16 screened tumor cell lines possessed a strong monocyte to Mϕ differentiating activity, which was totally due to tumor-derived M-CSF–secreted isoforms.

To identify novel molecules highly expressed in TC-Mϕ, we performed a gene expression analysis of these cells by Affymetrix technology, and we next compared these results to three other datasets of M1, M2, and TAM isolated from human tumors. Globally, the comparison of the four datasets confirmed that TC-Mϕ are indeed comparable to TAM and resemble more M2-Mϕ than M1-polarized cells. Among several common upregulated genes are the mannose receptor, other members of the C-type lectin R family, receptors for the Fc fragment of IgG, and receptors importantly implicated in the uptake and scavenging of debris, as well as several adhesion molecules.

In TC-Mϕ, the most expressed gene was *SEPP1*, a plasma transporter of selenium that has been implicated in the protection of tissues and in particular of endothelial cells from oxidative damage (63). In a recent study, SEPP1 was reported to be essential to limit disease severity of African trypanosome infection through its antioxidant activity (64). Within the tumor microenvironment, the presence of Mϕ-derived SEPP1 may protect tumor vessels, cancer cells, and Mϕ themselves from damage and consequently support tumor survival and growth. Our analysis shows that SEPP1 is highly expressed at the RNA level by M2-polarized Mϕ and TAM, but not by M1 cells, indicating that SEPP1 is a putative good marker of M2 cells. SEPP1 expression

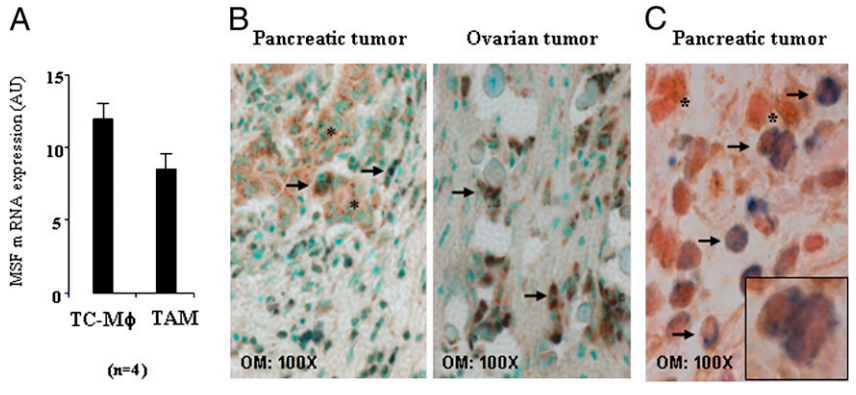

FIGURE 5. Expression of MSF in human TAMs. *A*, MSF mRNA expression in TAMs. Mean of four different donors. *B*, Immunohistochemistry of MSF (brown) in $CD68^+$ (blue) TAMs from pancreatic or ovarian tumors; nuclei are green. Arrows indicate $CD68^+MSF^+$ cells. *C*, Immunohistochemistry of MSF (brown) in $CD68^+$ (blue) TAM from pancreatic tumors (original magnification ×100). Nuclei are red. Arrows indicate $CD68^+MSF^+$ cells. *MSF-positive tumor cells.

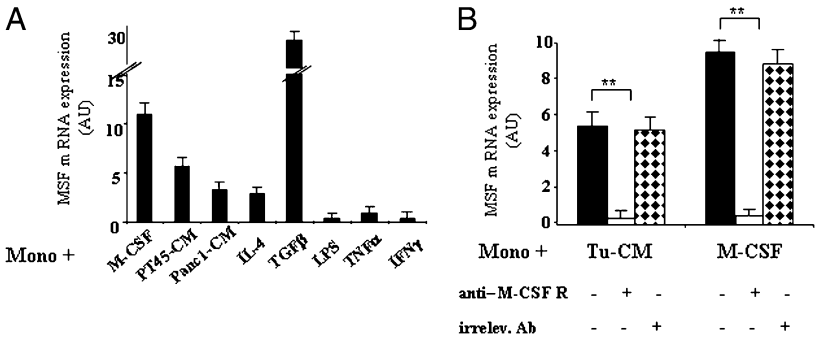

FIGURE 6. Modulation of MSF expression in monocytes. *A*, MSF mRNA expression in monocytes treated O/N with the indicated stimuli. *B*, Pretreatment of monocytes with anti–M-CSF Ab prestimulation with Panc1-CM for 24 h abrogated MSF expression. $**p \leq 0.01$.

is reduced in IL-10 knockout mice, indicating a role for IL-10 in its regulation (64).

Several upregulated genes were related to the ECM organization and turnover. ECM proteins are continuously produced and degraded by many cell types (tumor, endothelial, and stromal cells), among which TAM are master regulators. The incessant and dysregulated remodeling of the ECM in tumors leads to the aberrant presence of some matricellular components that are not usually found in normal tissues. In TC-Mϕ, we identified upregulated transglutaminase *F13A1*, which catalyzes the polymerization of several matrix proteins, *OA*, *OPN*, *FN1*, and proteolytic enzymes.

OA is a poorly characterized transmembrane molecule having supposed functions in cell adhesion, migration, and differentiation. Its expression has been linked to the upregulation of MMP3 and MMP9 in transformed astrocytes and fibroblasts (65, 66). In OA-transgenic mice, the molecule showed a cytoprotective effect on fibrosis induced by skeletal muscle denervation (67). These findings allow the hypothesis that OA could be involved in the pathophysiological cascade of tissue injury and repair. In addition, uremic Mϕ in patients with end-stage renal disease have been recently demonstrated to exhibit increased levels of this protein (68). OA was found overexpressed in various malignant tumors (65, 69, 70); moreover, it has been described that overexpression of OA in glioma and hepatoma cell lines sustains tumor invasiveness (65, 71). OA has an Arg-Gly-Asp integrin-binding domain; in mouse dendritic cells, OA enhances adhesion and transendothelial migration (72). The role of OA in myeloid cells infiltrating the tumor microenvironment is still unknown, but it could be speculatively linked to their efficient tissue remodeling function and MMP activation.

OPN has long attracted the interest of immunologists because of its many functions in inflammation, immunopathology, and hematopoiesis (73–78). Its expression is increased in response to cell injury or infections and is induced by a variety of proinflammatory mediators and growth factors such as IL-1, TNF-α, and platelet-derived growth factor (79). Elevated levels of OPN are associated with a remarkable variety of pathological processes ranging from atherosclerosis, autoimmune diseases, and cancer (74, 76, 79–81). A correlation between elevated OPN expression and malignant invasion (82–89) was suspected because OPN controls tumor cell motility and invasion through the engagement of CD44 receptors (90–92). Stromal cells and fibroblasts in particular are known to secrete OPN around tumor cell nests. Our study indicates that OPN was also highly expressed by TC-Mϕ.

We found FN upregulation in TC-Mϕ of special interest. FN is the most well-studied matrix protein, and it is known that in

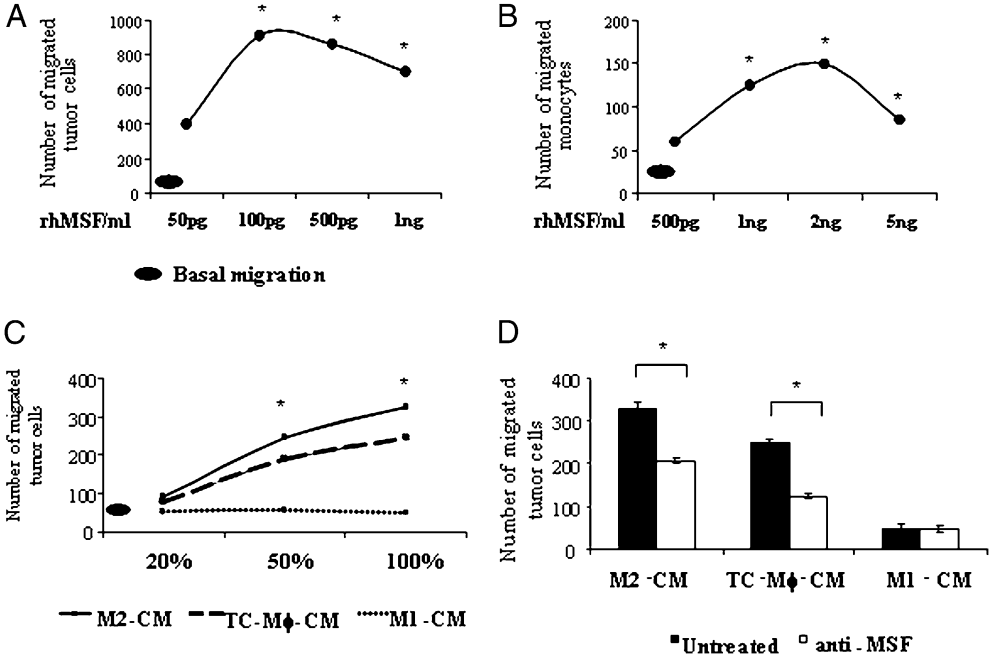

FIGURE 7. Chemotactic activity of rhMSF and TC-Mϕ–derived MSFs. Panc1 tumor cells (*A*) and monocytes (*B*) migration to rhMSF in transwell plates (18 h). Black circles indicate basal migration in the absence of MSF. *C*, CM from TC-Mϕ, M1-, and M2-polarized Mϕ was used as chemoattractant for Panc1 tumor cells at 20, 50, and 100% v/v. *D*, Inhibition of MSF with a specific anti–Gel-BD domain reduced the number of migrated tumor cells. $*p \leq 0.05$, significantly different compared with basal migration.

transformed cells and in malignancies, the splicing pattern of FN pre-mRNA becomes altered, leading to an increased expression of oncofoetal isoforms (93–95). The ED-A (59) and ED-B (96–98) are well-known oncofetal isoforms of FN. They are highly expressed in many tumors and promote cell spreading and angiogenesis (61, 93, 99). In particular, ED-B (96) is produced during active tissue remodeling like wound healing and, in tumor angiogenesis processes, gives rise to a prominent perivascular expression pattern (58).

A third oncofetal FN isoform, known as MSF, has been cloned in 2003 by Schor and colleagues. MSF differs from the other two oncofetal full-length isoforms because it is identical to their 70-kDa N terminus but terminates in a unique 10 aa sequence. Thus, MSF has been defined as truncated isoform (62). Unlike the angiogenic ED-A and ED-B, MSF was first identified by its motogenic activity in the CM of cultured fetal fibroblasts (100, 101). In this study, we show that TC-Mϕ produce MSF, whereas the ED-A and ED-B isoforms are not significantly expressed. MSF was known to be produced by fetal skin keratinocytes, neoplastic cells, and tumor-associated vascular endothelial cells (62), but has never been reported in Mϕ. It is also expressed during wound healing and strongly overexpressed in a wide range of common human cancers (62, 102). rMSF displays a number of potent bioactivities relevant to cancer development processes, including stimulation of cell migration, hyaluronan synthesis (103, 104), proteolytic activity (105), and angiogenesis (62, 102).

Of note, we observed an opposite trend over time for the MSF expression compared with full-length FN. TC-Mϕ–derived MSF increased along with either the time of culture or the number of supernatant stimuli, whereas transcripts from the full-length FN decreased. These data suggested a strict influence by the tumor microenvironment on FN isoform production. Importantly, MSF expression is upregulated in M2 compared with M1-Mϕ and MSF RNA and protein (immunohistochemistry) were found also in human TAMs. Thus, MSF may represent a good candidate marker of M2-Mϕ polarization and TAM.

In regards to its functions, due to its Gel-BD motogenic site, MSF had strong chemotactic activity for monocytes and tumor cells. Interestingly, this bioactivity is not expressed by full-length FN. It is known in fact that some biological activities of FN are acquired by denaturation and/or proteolytic cleavage. Schor et al. have reported that the Gel-BD domain is cryptic in full-length FN and acquires potent motogenic activity postproteolysis (62). Thus, two independent mechanisms for locally generating the same migratory activity are available in tissues: one by degradation of the extracellular matrix (Gel-BD) and the other by genetic control of FN truncation during gene transcription (MSF). The generation of MSF via a genetic mechanism is likely more efficient and does not rely on the activation of proteolytic enzymes; in addition, some cleaved FN fragments (e.g., Cell-BD) also have potent inhibitory effects on Gel-BD and MSF motogenic activity. We have shown in this study that MSF-containing supernatants of TC-Mϕ induced migration of both monocytes and tumor cells, underlining autocrine regulatory loops of leukocyte recruitment as well as paracrine effects on cancer cells. The observation that Mϕ secrete a chemotactic molecule that induces the migration of tumor cells highlights a new protumoral mechanism of these cells, already implicated in the process of distant metastasis and more recently in the preparation of the metastatic niche (23, 24, 106).

Another relevant consideration is MSF as therapeutic target. It was recently reported that the in vivo biodistribution of a labeled anti-MSF Ab was selectively concentrated in tumor vessels in a mouse model of xenograft esophageal carcinoma (107). Interestingly, administration of the anti-MSF Ab to tumor-bearing mice significantly reduced tumor growth, thus indicating that targeting of MSF in tumors may have therapeutic potential (107). Up to now, Mϕ markers with prognostic utility detectable in biological fluids of patients with cancer have been almost ignored. Of interest, MSF has been measured in a pilot study and detected in the sera of the majority of breast cancer patients but not of healthy subjects (101, 108).

In conclusion, we have described in this study that, in terms of gene profiling, TC-Mϕ are strongly comparable to TAMs and resemble M2-like polarized cells, thus confirming and boosting the concept of an M2-like polarization of tumor Mϕ. Among some interesting upregulated molecules, we focused on MSF, a truncated FN with motogenic activity. We suggest it as a new specific marker for M2-polarized Mϕ and TAM that might be considered in the design of anti-Mϕ approaches for novel anti-cancer therapies. Further studies are needed to elucidate the involvement of MSF in the protumoral role of Mϕ and as a biomarker in patients with cancer.

Acknowledgments

We thank Profs. Ana and Seth Schor (University of Dundee, Scotland, U.K.) for kindly providing recombinant human MSF and anti-MSF Abs. We also thank Dr. Giuseppe Peri for support and assistance during our anti-MSF Ab production and Dr. Federica Marchesi (Istituto Clinico Humanitas, Milan, Italy) and Dr. Fernando O. Martinez (University of Oxford, Oxford, U.K.) for help and suggestions.

Disclosures

The authors have no financial conflicts of interest.

References

1. Sica, A., T. Schioppa, A. Mantovani, and P. Allavena. 2006. Tumour-associated macrophages are a distinct M2 polarised population promoting tumour progression: potential targets of anti-cancer therapy. *Eur. J. Cancer* 42: 717–727.
2. Steidl, C., T. Lee, S. P. Shah, P. Farinha, G. Han, T. Nayar, A. Delaney, S. J. Jones, J. Iqbal, D. D. Weisenburger, et al. 2010. Tumor-associated macrophages and survival in classic Hodgkin's lymphoma. *N. Engl. J. Med.* 362: 875–885.
3. Condeelis, J., and J. W. Pollard. 2006. Macrophages: obligate partners for tumor cell migration, invasion, and metastasis. *Cell* 124: 263–266.
4. An, T., U. Sood, T. Pietruk, G. Cummings, K. Hashimoto, and J. D. Crissman. 1987. In situ quantitation of inflammatory mononuclear cells in ductal infiltrating breast carcinoma. Relation to prognostic parameters. *Am. J. Pathol.* 128: 52–60.
5. Bingle, L., N. J. Brown, and C. E. Lewis. 2002. The role of tumour-associated macrophages in tumour progression: implications for new anticancer therapies. *J. Pathol.* 196: 254–265.
6. Tsutsui, S., K. Yasuda, K. Suzuki, K. Tahara, H. Higashi, and S. Era. 2005. Macrophage infiltration and its prognostic implications in breast cancer: the relationship with VEGF expression and microvessel density. *Oncol. Rep.* 14: 425–431.
7. Pollard, J. W. 2008. Macrophages define the invasive microenvironment in breast cancer. *J. Leukoc. Biol.* 84: 623–630.
8. Paik, S., S. Shak, G. Tang, C. Kim, J. Baker, M. Cronin, F. L. Baehner, M. G. Walker, D. Watson, T. Park, et al. 2004. A multigene assay to predict recurrence of tamoxifen-treated, node-negative breast cancer. *N. Engl. J. Med.* 351: 2817–2826.
9. Dave, S. S., G. Wright, B. Tan, A. Rosenwald, R. D. Gascoyne, W. C. Chan, R. I. Fisher, R. M. Braziel, L. M. Rimsza, T. M. Grogan, et al. 2004. Prediction of survival in follicular lymphoma based on molecular features of tumor-infiltrating immune cells. *N. Engl. J. Med.* 351: 2159–2169.
10. Lin, E. Y., A. V. Nguyen, R. G. Russell, and J. W. Pollard. 2001. Colony-stimulating factor 1 promotes progression of mammary tumors to malignancy. *J. Exp. Med.* 193: 727–740.
11. Lazennec, G., and A. Richmond. 2010. Chemokines and chemokine receptors: new insights into cancer-related inflammation. *Trends Mol. Med.* 16: 133–144.
12. Solinas, G., G. Germano, A. Mantovani, and P. Allavena. 2009. Tumor-associated macrophages (TAM) as major players of the cancer-related inflammation. *J. Leukoc. Biol.* 86: 1065–1073.
13. DeNardo, D. G., M. Johansson, and L. M. Coussens. 2008. Immune cells as mediators of solid tumor metastasis. *Cancer Metastasis Rev.* 27: 11–18.
14. Mantovani, A., T. Schioppa, C. Porta, P. Allavena, and A. Sica. 2006. Role of tumor-associated macrophages in tumor progression and invasion. *Cancer Metastasis Rev.* 25: 315–322.
15. Pollard, J. W. 2004. Tumour-educated macrophages promote tumour progression and metastasis. *Nat. Rev. Cancer* 4: 71–78.

16. Talmadge, J. E., M. Donkor, and E. Scholar. 2007. Inflammatory cell infiltration of tumors: Jekyll or Hyde. *Cancer Metastasis Rev.* 26: 373–400.
17. Mantovani, A., P. Allavena, A. Sica, and F. Balkwill. 2008. Cancer-related inflammation. *Nature* 454: 436–444.
18. Hagemann, T., S. C. Robinson, M. Schulz, L. Trümper, F. R. Balkwill, and C. Binder. 2004. Enhanced invasiveness of breast cancer cell lines upon co-cultivation with macrophages is due to TNF-alpha dependent up-regulation of matrix metalloproteases. *Carcinogenesis* 25: 1543–1549.
19. Biswas, S. K., L. Gangi, S. Paul, T. Schioppa, A. Saccani, M. Sironi, B. Bottazzi, A. Doni, B. Vincenzo, F. Pasqualini, et al. 2006. A distinct and unique transcriptional program expressed by tumor-associated macrophages (defective NF-kappaB and enhanced IRF-3/STAT1 activation). *Blood* 107: 2112–2122.
20. Ojalvo, L. S., C. A. Whittaker, J. S. Condeelis, and J. W. Pollard. 2010. Gene expression analysis of macrophages that facilitate tumor invasion supports a role for Wnt-signaling in mediating their activity in primary mammary tumors. *J. Immunol.* 184: 702–712.
21. Joyce, J. A., and J. W. Pollard. 2009. Microenvironmental regulation of metastasis. *Nat. Rev. Cancer* 9: 239–252.
22. Erler, J. T., K. L. Bennewith, T. R. Cox, G. Lang, D. Bird, A. Koong, Q. T. Le, and A. J. Giaccia. 2009. Hypoxia-induced lysyl oxidase is a critical mediator of bone marrow cell recruitment to form the premetastatic niche. *Cancer Cell* 15: 35–44.
23. Hiratsuka, S., A. Watanabe, H. Aburatani, and Y. Maru. 2006. Tumour-mediated upregulation of chemoattractants and recruitment of myeloid cells predetermines lung metastasis. *Nat. Cell Biol.* 8: 1369–1375.
24. Kaplan, R. N., S. Rafii, and D. Lyden. 2006. Preparing the "soil": the pre-metastatic niche. *Cancer Res.* 66: 11089–11093.
25. Kaplan, R. N., R. D. Riba, S. Zacharoulis, A. H. Bramley, L. Vincent, C. Costa, D. D. MacDonald, D. K. Jin, K. Shido, S. A. Kerns, et al. 2005. VEGFR1-positive haematopoietic bone marrow progenitors initiate the pre-metastatic niche. *Nature* 438: 820–827.
26. Murdoch, C., M. Muthana, S. B. Coffelt, and C. E. Lewis. 2008. The role of myeloid cells in the promotion of tumour angiogenesis. *Nat. Rev. Cancer* 8: 618–631.
27. Padua, D., X. H. Zhang, Q. Wang, C. Nadal, W. L. Gerald, R. R. Gomis, and J. Massagué. 2008. TGFbeta primes breast tumors for lung metastasis seeding through angiopoietin-like 4. *Cell* 133: 66–77.
28. Mantovani, A., S. Sozzani, M. Locati, P. Allavena, and A. Sica. 2002. Macrophage polarization: tumor-associated macrophages as a paradigm for polarized M2 mononuclear phagocytes. *Trends Immunol.* 23: 549–555.
29. Ghassabeh, G. H., P. De Baetselier, L. Brys, W. Noël, J. A. Van Ginderachter, S. Meerschaut, A. Beschin, F. Brombacher, and G. Raes. 2006. Identification of a common gene signature for type II cytokine-associated myeloid cells elicited in vivo in different pathologic conditions. *Blood* 108: 575–583.
30. Nevala, W. K., C. M. Vachon, A. A. Leontovich, C. G. Scott, M. A. Thompson, and S. N. Markovic; Melanoma Study Group of the Mayo Clinic Cancer Center. 2009. Evidence of systemic Th2-driven chronic inflammation in patients with metastatic melanoma. *Clin. Cancer Res.* 15: 1931–1939.
31. Deepak, P., S. Kumar, and A. Acharya. 2007. Interleukin-13-induced type II polarization of inflammatory macrophages is mediated through suppression of nuclear factor-kappaB and preservation of IkappaBalpha in a T cell lymphoma. [Published retraction appears in 2009 *Clin. Exp. Immunol.* 158: 334.] *Clin. Exp. Immunol.* 149: 378–386.
32. Cheadle, E. J., K. Riyad, D. Subar, D. G. Rothwell, G. Ashton, H. Batha, D. J. Sherlock, R. E. Hawkins, and D. E. Gilham. 2007. Eotaxin-2 and colorectal cancer: a potential target for immune therapy. *Clin. Cancer Res.* 13: 5719–5728.
33. DeNardo, D. G., J. B. Barreto, P. Andreu, L. Vasquez, D. Tawfik, N. Kolhatkar, and L. M. Coussens. 2009. CD4(+) T cells regulate pulmonary metastasis of mammary carcinomas by enhancing protumor properties of macrophages. *Cancer Cell* 16: 91–102.
34. Goerdt, S., and C. E. Orfanos. 1999. Other functions, other genes: alternative activation of antigen-presenting cells. *Immunity* 10: 137–142.
35. Gabrilovich, D. I., and S. Nagaraj. 2009. Myeloid-derived suppressor cells as regulators of the immune system. *Nat. Rev. Immunol.* 9: 162–174.
36. Gordon, S., and P. R. Taylor. 2005. Monocyte and macrophage heterogeneity. *Nat. Rev. Immunol.* 5: 953–964.
37. Gordon, S. 2003. Alternative activation of macrophages. *Nat. Rev. Immunol.* 3: 23–35.
38. Mantovani, A., A. Sica, and M. Locati. 2005. Macrophage polarization comes of age. *Immunity* 23: 344–346.
39. Martinez, F. O., L. Helming, and S. Gordon. 2009. Alternative activation of macrophages: an immunologic functional perspective. *Annu. Rev. Immunol.* 27: 451–483.
40. Van Ginderachter, J. A., K. Movahedi, G. Hassanzadeh Ghassabeh, S. Meerschaut, A. Beschin, G. Raes, and P. De Baetselier. 2006. Classical and alternative activation of mononuclear phagocytes: picking the best of both worlds for tumor promotion. *Immunobiology* 211: 487–501.
41. Saccani, A., T. Schioppa, C. Porta, S. K. Biswas, M. Nebuloni, L. Vago, B. Bottazzi, M. P. Colombo, A. Mantovani, and A. Sica. 2006. p50 nuclear factor-kappaB overexpression in tumor-associated macrophages inhibits M1 inflammatory responses and antitumor resistance. *Cancer Res.* 66: 11432–11440.
42. Porta, C., M. Rimoldi, G. Raes, L. Brys, P. Ghezzi, D. Di Liberto, F. Dieli, S. Ghisletti, G. Natoli, P. De Baetselier, et al. 2009. Tolerance and M2 (alternative) macrophage polarization are related processes orchestrated by p50 nuclear factor kappaB. *Proc. Natl. Acad. Sci. USA* 106: 14978–14983.
43. Bouhlel, M. A., B. Derudas, E. Rigamonti, R. Dièvart, J. Brozek, S. Haulon, C. Zawadzki, B. Jude, G. Torpier, N. Marx, et al. 2007. PPARgamma activation primes human monocytes into alternative M2 macrophages with anti-inflammatory properties. *Cell Metab.* 6: 137–143.
44. Van Ginderachter, J. A., K. Movahedi, J. Van den Bossche, and P. De Baetselier. 2008. Macrophages, PPARs, and Cancer. *PPAR Res.* 2008: 169414.
45. Van Ginderachter, J. A., S. Meerschaut, Y. Liu, L. Brys, K. De Groeve, G. Hassanzadeh Ghassabeh, G. Raes, and P. De Baetselier. 2006. Peroxisome proliferator-activated receptor gamma (PPARgamma) ligands reverse CTL suppression by alternatively activated (M2) macrophages in cancer. *Blood* 108: 525–535.
46. Odegaard, J. I., R. R. Ricardo-Gonzalez, M. H. Goforth, C. R. Morel, V. Subramanian, L. Mukundan, A. Red Eagle, D. Vats, F. Brombacher, A. W. Ferrante, and A. Chawla. 2007. Macrophage-specific PPARgamma controls alternative activation and improves insulin resistance. *Nature* 447: 1116–1120.
47. Kuroda, E., V. Ho, J. Ruschmann, F. Antignano, M. Hamilton, M. J. Rauh, A. Antov, R. A. Flavell, L. M. Sly, and G. Krystal. 2009. SHIP represses the generation of IL-3-induced M2 macrophages by inhibiting IL-4 production from basophils. *J. Immunol.* 183: 3652–3660.
48. Roca, H., Z. S. Varsos, S. Sud, M. J. Craig, C. Ying, and K. J. Pienta. 2009. CCL2 and interleukin-6 promote survival of human CD11b+ peripheral blood mononuclear cells and induce M2-type macrophage polarization. *J. Biol. Chem.* 284: 34342–34354.
49. Perrier, P., F. O. Martinez, M. Locati, G. Bianchi, M. Nebuloni, G. Vago, F. Bazzoni, S. Sozzani, P. Allavena, and A. Mantovani. 2004. Distinct transcriptional programs activated by interleukin-10 with or without lipopolysaccharide in dendritic cells: induction of the B cell-activating chemokine, CXC chemokine ligand 13. *J. Immunol.* 172: 7031–7042.
50. Jolliffe, I. T. 2002. *Principal Component Analysis.* Springer, New York.
51. Pixley, F. J., and E. R. Stanley. 2004. CSF-1 regulation of the wandering macrophage: complexity in action. *Trends Cell Biol.* 14: 628–638.
52. Kzhyshkowska, J., S. Mamidi, A. Gratchev, E. Kremmer, C. Schmuttermaier, L. Krusell, G. Haus, J. Utikal, K. Schledzewski, J. Scholtze, and S. Goerdt. 2006. Novel stabilin-1 interacting chitinase-like protein (SI-CLP) is up-regulated in alternatively activated macrophages and secreted via lysosomal pathway. *Blood* 107: 3221–3228.
53. Martinez, F. O., S. Gordon, M. Locati, and A. Mantovani. 2006. Transcriptional profiling of the human monocyte-to-macrophage differentiation and polarization: new molecules and patterns of gene expression. *J. Immunol.* 177: 7303–7311.
54. Raychaudhuri, S., J. M. Stuart, and R. B. Altman. 2000. Principal components analysis to summarize microarray experiments: application to sporulation time series. *Pac. Symp. Biocomput.* 5: 455–466.
55. Reiner, A., D. Yekutieli, and Y. Benjamini. 2003. Identifying differentially expressed genes using false discovery rate controlling procedures. *Bioinformatics* 19: 368–375.
56. Astrof, S., and R. O. Hynes. 2009. Fibronectins in vascular morphogenesis. *Angiogenesis* 12: 165–175.
57. Balza, E., F. Sassi, E. Ventura, A. Parodi, S. Fossati, W. Blalock, B. Carnemolla, P. Castellani, L. Zardi, and L. Borsi. 2009. A novel human fibronectin cryptic sequence unmasked by the insertion of the angiogenesis-associated extra type III domain B. *Int. J. Cancer* 125: 751–758.
58. Ffrench-Constant, C., L. Van de Water, H. F. Dvorak, and R. O. Hynes. 1989. Reappearance of an embryonic pattern of fibronectin splicing during wound healing in the adult rat. *J. Cell Biol.* 109: 903–914.
59. Kornblihtt, A. R., C. G. Pesce, C. R. Alonso, P. Cramer, A. Srebrow, S. Werbajh, and A. F. Muro. 1996. The fibronectin gene as a model for splicing and transcription studies. *FASEB J.* 10: 248–257.
60. Castellani, P., G. Viale, A. Dorcaratto, G. Nicolo, J. Kaczmarek, G. Querze, and L. Zardi. 1994. The fibronectin isoform containing the ED-B oncofetal domain: a marker of angiogenesis. *Int. J. Cancer* 59: 612–618.
61. Labat-Robert, J. 2002. Fibronectin in malignancy. *Semin. Cancer Biol.* 12: 187–195.
62. Schor, S. L., I. R. Ellis, S. J. Jones, R. Baillie, K. Seneviratne, J. Clausen, K. Motegi, B. Vojtesek, K. Kankova, E. Furrie, et al. 2003. Migration-stimulating factor: a genetically truncated onco-fetal fibronectin isoform expressed by carcinoma and tumor-associated stromal cells. *Cancer Res.* 63: 8827–8836.
63. Steinbrenner, H., and H. Sies. 2009. Protection against reactive oxygen species by selenoproteins. *Biochim. Biophys. Acta* 1790: 1478–1485.
64. Bosschaerts, T., M. Guilliams, W. Noel, M. Hérin, R. F. Burk, K. E. Hill, L. Brys, G. Raes, G. H. Ghassabeh, P. De Baetselier, and A. Beschin. 2008. Alternatively activated myeloid cells limit pathogenicity associated with African trypanosomiasis through the IL-10 inducible gene selenoprotein P. *J. Immunol.* 180: 6168–6175.
65. Rich, J. N., Q. Shi, M. Hjelmeland, T. J. Cummings, C. T. Kuan, D. D. Bigner, C. M. Counter, and X. F. Wang. 2003. Bone-related genes expressed in advanced malignancies induce invasion and metastasis in a genetically defined human cancer model. *J. Biol. Chem.* 278: 15951–15957.
66. Ogawa, T., T. Nikawa, H. Furochi, M. Kosyoji, K. Hirasaka, N. Suzue, K. Sairyo, S. Nakano, T. Yamaoka, M. Itakura, et al. 2005. Osteoactivin upregulates expression of MMP-3 and MMP-9 in fibroblasts infiltrated into denervated skeletal muscle in mice. *Am. J. Physiol. Cell Physiol.* 289: C697–C707.
67. Furochi, H., S. Tamura, K. Takeshima, K. Hirasaka, R. Nakao, K. Kishi, and T. Nikawa. 2007. Overexpression of osteoactivin protects skeletal muscle from

severe degeneration caused by long-term denervation in mice. *J. Med. Invest.* 54: 248–254.
68. Pahl, M. V., N. D. Vaziri, J. Yuan, and S. G. Adler. 2010. Upregulation of monocyte/macrophage HGFIN (Gpnmb/Osteoactivin) expression in end-stage renal disease. *Clin. J. Am. Soc. Nephrol.* 5: 56–61.
69. Weterman, M. A., N. Ajubi, I. M. van Dinter, W. G. Degen, G. N. van Muijen, D. J. Ruitter, and H. P. Bloemers. 1995. nmb, a novel gene, is expressed in low-metastatic human melanoma cell lines and xenografts. *Int. J. Cancer* 60: 73–81.
70. Loging, W. T., A. Lal, I. M. Siu, T. L. Loney, C. J. Wikstrand, M. A. Marra, C. Prange, D. D. Bigner, R. L. Strausberg, and G. J. Riggins. 2000. Identifying potential tumor markers and antigens by database mining and rapid expression screening. *Genome Res.* 10: 1393–1402.
71. Onaga, M., A. Ido, S. Hasuike, H. Uto, A. Moriuchi, K. Nagata, T. Hori, K. Hayash, and H. Tsubouchi. 2003. Osteoactivin expressed during cirrhosis development in rats fed a choline-deficient, L-amino acid-defined diet, accelerates motility of hepatoma cells. *J. Hepatol.* 39: 779–785.
72. Shikano, S., M. Bonkobara, P. K. Zukas, and K. Ariizumi. 2001. Molecular cloning of a dendritic cell-associated transmembrane protein, DC-HIL, that promotes RGD-dependent adhesion of endothelial cells through recognition of heparan sulfate proteoglycans. *J. Biol. Chem.* 276: 8125–8134.
73. Haylock, D. N., and S. K. Nilsson. 2006. Osteopontin: a bridge between bone and blood. *Br. J. Haematol.* 134: 467–474.
74. O'Regan, A. W., G. J. Nau, G. L. Chupp, and J. S. Berman. 2000. Osteopontin (Eta-1) in cell-mediated immunity: teaching an old dog new tricks. *Immunol. Today* 21: 475–478.
75. Shinohara, M. L., L. Lu, J. Bu, M. B. Werneck, K. S. Kobayashi, L. H. Glimcher, and H. Cantor. 2006. Osteopontin expression is essential for interferon-alpha production by plasmacytoid dendritic cells. *Nat. Immunol.* 7: 498–506.
76. Rangaswami, H., A. Bulbule, and G. C. Kundu. 2006. Osteopontin: role in cell signaling and cancer progression. *Trends Cell Biol.* 16: 79–87.
77. Shinohara, M. L., M. Jansson, E. S. Hwang, M. B. Werneck, L. H. Glimcher, and H. Cantor. 2005. T-bet-dependent expression of osteopontin contributes to T cell polarization. *Proc. Natl. Acad. Sci. USA* 102: 17101–17106.
78. Diao, H., S. Kon, K. Iwabuchi, C. Kimura, J. Morimoto, D. Ito, T. Segawa, M. Maeda, J. Hamuro, T. Nakayama, et al. 2004. Osteopontin as a mediator of NKT cell function in T cell-mediated liver diseases. *Immunity* 21: 539–550.
79. Denhardt, D. T., M. Noda, A. W. O'Regan, D. Pavlin, and J. S. Berman. 2001. Osteopontin as a means to cope with environmental insults: regulation of inflammation, tissue remodeling, and cell survival. *J. Clin. Invest.* 107: 1055–1061.
80. Scatena, M., L. Liaw, and C. M. Giachelli. 2007. Osteopontin: a multifunctional molecule regulating chronic inflammation and vascular disease. *Arterioscler. Thromb. Vasc. Biol.* 27: 2302–2309.
81. Hur, E. M., S. Youssef, M. E. Haws, S. Y. Zhang, R. A. Sobel, and L. Steinman. 2007. Osteopontin-induced relapse and progression of autoimmune brain disease through enhanced survival of activated T cells. *Nat. Immunol.* 8: 74–83.
82. Senger, D. R., C. A. Perruzzi, C. F. Gracey, A. Papadopoulos, and D. G. Tenen. 1988. Secreted phosphoproteins associated with neoplastic transformation: close homology with plasma proteins cleaved during blood coagulation. *Cancer Res.* 48: 5770–5774.
83. Brown, L. F., A. Papadopoulos-Sergiou, B. Berse, E. J. Manseau, K. Tognazzi, C. A. Perruzzi, H. F. Dvorak, and D. R. Senger. 1994. Osteopontin expression and distribution in human carcinomas. *Am. J. Pathol.* 145: 610–623.
84. Bellahcène, A., and V. Castronovo. 1995. Increased expression of osteonectin and osteopontin, two bone matrix proteins, in human breast cancer. *Am. J. Pathol.* 146: 95–100.
85. Hirota, S., A. Ito, J. Nagoshi, M. Takeda, A. Kurata, Y. Takatsuka, K. Kohri, S. Nomura, and Y. Kitamura. 1995. Expression of bone matrix protein messenger ribonucleic acids in human breast cancers. Possible involvement of osteopontin in development of calcifying foci. *Lab. Invest.* 72: 64–69.
86. Singhal, H., D. S. Bautista, K. S. Tonkin, F. P. O'Malley, A. B. Tuck, A. F. Chambers, and J. F. Harris. 1997. Elevated plasma osteopontin in metastatic breast cancer associated with increased tumor burden and decreased survival. *Clin. Cancer Res.* 3: 605–611.
87. Tuck, A. B., F. P. O'Malley, H. Singhal, J. F. Harris, K. S. Tonkin, N. Kerkvliet, Z. Saad, G. S. Doig, and A. F. Chambers. 1998. Osteopontin expression in a group of lymph node negative breast cancer patients. *Int. J. Cancer* 79: 502–508.
88. Casson, A. G., S. M. Wilson, J. A. McCart, F. P. O'Malley, H. Ozcelik, M. S. Tsao, and A. F. Chambers. 1997. ras mutation and expression of the ras-regulated genes osteopontin and cathepsin L in human esophageal cancer. *Int. J. Cancer* 72: 739–745.
89. Gotoh, M., M. Sakamoto, K. Kanetaka, M. Chuuma, and S. Hirohashi. 2002. Overexpression of osteopontin in hepatocellular carcinoma. *Pathol. Int.* 52: 19–24.
90. Kazanecki, C. C., D. J. Uzwiak, and D. T. Denhardt. 2007. Control of osteopontin signaling and function by post-translational phosphorylation and protein folding. *J. Cell. Biochem.* 102: 912–924.
91. Liaw, L., M. P. Skinner, E. W. Raines, R. Ross, D. A. Cheresh, S. M. Schwartz, and C. M. Giachelli. 1995. The adhesive and migratory effects of osteopontin are mediated via distinct cell surface integrins. Role of alpha v beta 3 in smooth muscle cell migration to osteopontin in vitro. *J. Clin. Invest.* 95: 713–724.
92. Weber, G. F., S. Ashkar, M. J. Glimcher, and H. Cantor. 1996. Receptor-ligand interaction between CD44 and osteopontin (Eta-1). *Science* 271: 509–512.
93. Kaczmarek, J., P. Castellani, G. Nicolo, B. Spina, G. Allemanni, and L. Zardi. 1994. Distribution of oncofetal fibronectin isoforms in normal, hyperplastic and neoplastic human breast tissues. *Int. J. Cancer* 59: 11–16.
94. Oyama, F., S. Hirohashi, Y. Shimosato, K. Titani, and K. Sekiguchi. 1990. Oncodevelopmental regulation of the alternative splicing of fibronectin premessenger RNA in human lung tissues. *Cancer Res.* 50: 1075–1078.
95. Oyama, F., S. Hirohashi, Y. Shimosato, K. Titani, and K. Sekiguchi. 1989. Deregulation of alternative splicing of fibronectin pre-mRNA in malignant human liver tumors. *J. Biol. Chem.* 264: 10331–10334.
96. Zardi, L., B. Carnemolla, A. Siri, T. E. Petersen, G. Paolella, G. Sebastio, and F. E. Baralle. 1987. Transformed human cells produce a new fibronectin isoform by preferential alternative splicing of a previously unobserved exon. *EMBO J.* 6: 2337–2342.
97. Schwarzbauer, J. E., R. S. Patel, D. Fonda, and R. O. Hynes. 1987. Multiple sites of alternative splicing of the rat fibronectin gene transcript. *EMBO J.* 6: 2573–2580.
98. Gutman, A., and A. R. Kornblihtt. 1987. Identification of a third region of cell-specific alternative splicing in human fibronectin mRNA. *Proc. Natl. Acad. Sci. USA* 84: 7179–7182.
99. Midulla, M., R. Verma, M. Pignatelli, M. A. Ritter, N. S. Courtenay-Luck, and A. J. George. 2000. Source of oncofetal ED-B-containing fibronectin: implications of production by both tumor and endothelial cells. *Cancer Res.* 60: 164–169.
100. Schor, S. L., A. M. Schor, G. Rushton, and L. Smith. 1985. Adult, foetal and transformed fibroblasts display different migratory phenotypes on collagen gels: evidence for an isoformic transition during foetal development. *J. Cell Sci.* 73: 221–234.
101. Schor, S. L., A. M. Schor, A. M. Grey, and G. Rushton. 1988. Foetal and cancer patient fibroblasts produce an autocrine migration-stimulating factor not made by normal adult cells. *J. Cell Sci.* 90: 391–399.
102. Schor, S. L., and A. M. Schor. 2001. Phenotypic and genetic alterations in mammary stroma: implications for tumour progression. *Breast Cancer Res.* 3: 373–379.
103. Schor, S. L., A. M. Schor, A. M. Grey, J. Chen, G. Rushton, M. E. Grant, and I. Ellis. 1989. Mechanism of action of the migration stimulating factor produced by fetal and cancer patient fibroblasts: effect on hyaluronic and synthesis. *In Vitro Cell. Dev. Biol.* 25: 737–746.
104. Ellis, I., A. M. Grey, A. M. Schor, and S. L. Schor. 1992. Antagonistic effects of TGF-beta 1 and MSF on fibroblast migration and hyaluronic acid synthesis. Possible implications for dermal wound healing. *J. Cell Sci.* 102: 447–456.
105. Houard, X., S. Germain, M. Gervais, A. Michaud, F. van den Brûle, J. M. Foidart, A. Noël, C. Monnot, and P. Corvol. 2005. Migration-stimulating factor displays HEXXH-dependent catalytic activity important for promoting tumor cell migration. *Int. J. Cancer* 116: 378–384.
106. Qian, B., Y. Deng, J. H. Im, R. J. Muschel, Y. Zou, J. Li, R. A. Lang, and J. W. Pollard. 2009. A distinct macrophage population mediates metastatic breast cancer cell extravasation, establishment and growth. *PLoS ONE* 4: e6562.
107. Hu, H., Y. Ran, Y. Zhang, Z. Zhou, S. J. Harris, L. Yu, L. Sun, J. Pan, J. Liu, J. Lou, and Z. Yang. 2009. Antibody library-based tumor endothelial cells surface proteomic functional screen reveals migration-stimulating factor as an anti-angiogenic target. *Mol. Cell. Proteomics* 8: 816–826.
108. Picardo, M., S. L. Schor, A. M. Grey, A. Howell, I. Laidlaw, J. Redford, and A. M. Schor. 1991. Migration stimulating activity in serum of breast cancer patients. *Lancet* 337: 130–133.